INSIGHT. M. P. Panning¹, B. Knapmeyer-Endrun², F. Bissig³, R. Joshi⁴, A. Khan^{3,23}, D. Kim⁶, V. Lekić⁶, B. Tauzin⁷, S. Tharimena^{1,8}, M. Plasman⁹, N. Compaire¹⁰, R. F. Garcia¹⁰, L. Margerin¹¹, M. Schimmel¹², É. Stutzmann⁹, N.

SEISMIC CONSTRAINTS ON THE THICKNESS AND STRUCTURE OF THE MARTIAN CRUST FROM

Schmerr⁶, E. Bozdağ¹³, A.-C. Plesa¹⁴, M. A. Wieczorek¹⁵, A. Broquet¹⁵, D. Antonangeli¹⁶, S. M. McLennan¹⁷, H. Samuel⁹, C. Michaut^{7,18} L. Pan⁷, C. Perrin^{9,19}, S. E. Smrekar², C. L. Johnson^{20,21}, N. Brinkman³, A. Mittelholz³, A. Rivoldini²², P. M. Davis¹⁸, P. Lognonné^{9,23}, B. Pinot¹⁰, J.-R. Scholz⁴, S. C. Stähler³, M. Knapmeyer¹⁴, M. van Driel³, D. Giardini³, W. B. Banerdt¹; ¹Jet Propulsion Laboratory, California Institute of Technology, ²Bensberg Observatory, University of Cologne, ³ETH Zürich, ⁴Max Planck Institute for Solar System Research, ⁵University of Zürich, ⁶University of Maryland, ⁷Université de Lyon, ⁸now at University of Vienna, ⁹Université de Paris, Institut de Physique du Globe de Paris, CNRS, ¹⁰ISAE SUPAERO, ¹¹IRAP, Université Toulouse III Paul Sabatier, ¹²Geosciences Barcelona - CSIC, ¹³Colorado School of Mines, ¹⁴Institute of Planetary Research, German Aerospace Center (DLR), ¹⁵Université Côte d'Azur, ¹⁶IMPMC, Sorbonne Université, ¹⁷Stony Brook University, ¹⁸UCLA, ¹⁹now at Universite de Nantes, ²⁰University of British Columbia, ²¹Planetary Science Institute, ²²Royal Observatory of Belgium, ²³Institut Universitaire de France.

Introduction: NASA's InSight mission [1] has for the first time placed a very broad-band seismometer on the surface of Mars. The Seismic Experiment for Interior Structure (SEIS) [2] has been collecting continuous data since early February 2019. The main focus of InSight is to enhance our understanding of the internal structure and dynamics of Mars, which includes the goal to better constrain the crustal thickness of the planet [3]. Knowing the present-day crustal thickness of Mars has important implications for its thermal evolution [4] as well as for the partitioning of silicates and heat-producing elements between the different layers of Mars. Current estimates for the crustal thickness of Mars are based on modeling the relationship between topography and gravity [5,6], but these studies rely on different assumptions, e.g. on the density of the crust and upper mantle, or the bulk silicate composition of the planet and the crust. The resulting values for the average crustal thickness differ by more than 100%, from 30 km to more than 100 km [7].

New independent constraints from InSight will be based on seismically determining the crustal thickness at the landing site. This single firm measurement of crustal thickness at one point on the planet will allow to constrain both the average crustal thickness of Mars as well as thickness variations across the planet when combined with constraints from gravity and topography [8]. Here we describe the determination of the crustal structure and thickness at the InSight landing site based on seismic receiver functions for three marsquakes compared with autocorrelations of InSight data [9].

Methodology: For more than 40 years, receiver functions have become a powerful tool to study the crustal and upper mantle structure in terrestrial seismology [10-12]. The method isolates converted phases, either P-to-S conversions in the P-wave coda or S-to-P precursors to the S-wave, from teleseismic earthquakes by rotation into the ray coordinate system

and removal of the source-time-function, distant path effects, and the instrument response (Fig. 1). The relative travel-time of these phases in relation to the parent phase contains information on the depth of the layer where the conversion originates and the seismic velocities above. The receiver functions method has also been applied to data from one station of the Apollo lunar seismic network, though with different interpretations in terms of crustal thickness [13,14].

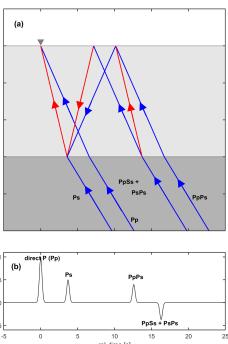


Figure 1: Schematic illustration of P-to-S phase conversions at a discontinuity (a) and corresponding receiver function (b)

We have calculated P-to-S receiver functions for three marsquakes and S-to-P receiver functions for two marsquakes. All of these quakes are located at comparatively small epicentral distances, between 25° and 46°. Results for different processing schemes (i.e. filtering, determination of rotation angles, deconvolution method) applied by different teams lead to similar results. As one of the quake recordings was also contaminated by a prominent glitch in the P-wave coda, we also compared results for different deglitching methods for this event to make sure we only interpret reliable phases [15].

We also calculate autocorrelation of seismic noise records and event codas, which can be used to approximate zero-offset vertical reflection response [16,17,18] and compare the predicted reflections from our receiver function inversions with prominent arrivals in autocorrelation functions, as well as comparing with published autocorrelation studies of InSight data [19].

Results: We observe consistent phases within the first 10 seconds of the P-to-S receiver functions. Within this time window, the energy level on the transverse component is low, indicating a minor role of anisotropy or scattering. At later times, consistency between different events and analysts is decreasing. The S-to-P receiver functions also show a consistent first phase. Later arrivals are harder to pinpoint, which could be due to the comparatively shallow incidence of the S-waves at the considered distances, which prevents the generation of converted waves. Inversions of the receiver functions are consistent with either a 2- or 3crustal model, allowing two possible interpretations of the crustal thickness. We also evaluate the implications for local crustal thickness at the InSight landing site for global crustal thickness [20] and consider implications for thermal evolution and concentrations of heat-producing elements in the crust [21].

Acknowledgments: We acknowledge NASA, CNES, partner agencies and institutions (UKSA, SSO, DLR, JPL, IPGP-CNRS, ETHZ, IC, MPS-MPG) and the operators of JPL, SISMOC, MSDS, IRIS-DMC and PDS for providing SEED SEIS data. InSight data is archived in the PDS, and a full list of archives in the Geosciences, Atmospheres, and Imaging nodes is at https://pds-geosciences.wustl.edu/missions/insight/.

This work was partially carried out at the Jet Propulsion Laboratory, California Institute of Technology, under a contract with the National Aeronautics and Space Administration. ©2021, California Institute of Technology, Government sponsorship acknowledged.

References: [1] Banerdt, W.B. et al. (2020) *Nature Geo.*, 13, 183. [2] Longonné et al. (2019) Space Sci. Rev., 215, 12 [3] Smrekar S. E. et al. (2019) *Space Sci*

Rev, 215, 3. [4] Plesa A.-C. et al. (2018) GRL, 45, 2580-2589. [5] Neumann G. A. et al. (2004) JGR, 109, E08002. [6] Wieczorek M. A. and Zuber M. T. (2004) JGR, 109, E01009. [7] Baratoux D. et al. (2014) JGR, 119, 1707-1727. [8] Wieczorek M. A. et al. (2020) LPS LI. [9] InSight Mars SEIS Data Service (2019) https://doi.org/10.18715/SEIS. INSIGHT.XB 2016 [10] Langston C. A. (1979) JGR, 84, 4749-4762. [11] Lawrence J. F. and Shearer P. M. (2006) JGR, 111, B06307 [12] Abt D. L. et al. (2010) JGR, 115, B09301. [13] Vinnik L. et al. (2001) GRL, 28, 3031-3034 [14] Lognonné P. et al. (2003), EPSL, 211, 27-44. [15] Lognonné P. et al. (2020) Nature Geo., 13, 213. [16] Wapenaar, K. et al. (2010) Geophysics, 75, 75A195. [17] Kim, D. and Lekić, V. (2019) Geophys. Res. Lett., 46, 13722. [18] Schimmel M. et al. (2018) Seism. Res. Lett., 89, 1488. [19] Deng, S. and Levander, A. (2020) Geophys. Res. Lett., 47, e2020GL089630. [20] Wieczorek, M. A. et al. (2021) LPSC. [21] Michaut, C. et al. (2021) LPSC.